S-Parameter Formulation of Quality Factor for a Spiral Inductor in Generalized Two-Port Configuration

T.S. Horng, K.C. Peng, J.K. Jau, and Y.S. Tsai

Department of Electrical Engineering, National Sun Yat-Sen University, Kaohsiung, 804, Taiwan

Abstract — **In this paper, we present the most rigorous S-parameter formulation of quality (Q) factor that has ever been seen for a spiral inductor in generalized two-port configuration. The derivation employs a complex power concept and can reduce to the conventional Q-factor expression based on one-port inductor model with the second port grounded. The Q factor of a tank circuit that connects the spiral inductor with an ideally lossless capacitor in series or in parallel can be also predicted successfully using this S-parameter formulation.**

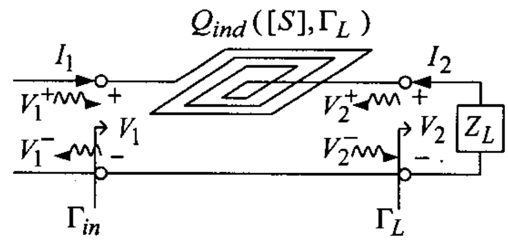

Fig.1. Microwave network representation of a spiral inductor in two-port configuration.

I. INTRODUCTION

Spiral inductors are commonly used in radio-frequency integrated circuits (RFICs) to act as series or shunt elements in the matching, tank or choke circuits. It is without controversy that Q factor is always the most important parameter to evaluate the inductor performance. However, up to date the spiral-inductor Q factor has been formulated rigorously as the ratio of imaginary part to real part of input impedance only in one port configuration with another port shorted [1]-[3]. This Q-factor formulation is good for spiral inductors when serving as shunt elements. Spiral inductors are also used frequently as series elements in many RFIC applications and their performance will be distorted when evaluated using the Q factor in one-port formulation. Several Q factors have been calculated based on various two-port inductor models in the past [4],[5]. It is common for them to ignore the loss of the shunt parasitic elements in the model, which will generally lead to overestimation of Q factors below self-resonant frequency (SRF).

In this paper, we consider the spiral inductor as a reciprocal two-port network. According to a general relation between its impedance network parameters and the complex power delivered to this network, we have derived a closed-form expression for Q factor in terms of two-port S parameters and load reflection coefficient successfully. By setting minus unity for load reflection coefficient to represent a short-circuit termination, the reduced expression of Q factor can be proved identical to that formulated in one-port configuration. A spiral inductor and a metal-insulator-metal (MIM) capacitor in series or parallel connection form fundamental tank circuits in RFICs. Typically, the former Q factor is much lower than the latter and will dominate the final Q factor of tank circuit. Therefore, it can be acceptable to assume an infinite Q-factor quantity for MIM capacitor in estimating Q factor of a tank circuit. By distinguishing the Q-factor definition between spiral inductor and tank circuit, we have found an approximate formula to predict the tank-circuit Q factor accurately from the spiral-inductor Q factor.

II. FORMULATION

By referring to [1]-[3], the spiral-inductor Q factor can be defined as

$$Q_{ind} = 2\pi \frac{\text{peak magnetic energy - peak electric energy}}{\text{energy loss in one cycle}}$$

$$= 2\pi \frac{(2W_m^{av} - 2W_e^{av})}{P_l^{av} \cdot T} = 2\omega \frac{(W_m^{av} - W_e^{av})}{P_l^{av}} \qquad (1)$$

where W_m^{av} and W_e^{av} are time-average magnetic and electric energy respectively and each is equal to half of its peak energy. The time-average power loss denoted by P_l^{av} should equal the energy loss in one cycle divided by the period (T). Fig. 1 shows a spiral inductor terminated by arbitrary load impedance (Z_L). From Poynting's theorem, the complex power delivered to the input of the network can be expressed in terms of the net reactive energy stored in and the power dissipated by the network. That is

0-7803-7694-3/03/$17.00 © 2003 IEEE

$$P_{av} = \frac{1}{2}[V]^t[I]^* = P_l^{av} + 2j\omega(W_m^{av} - W_e^{av}) \qquad (2)$$

where

$$[V] = [V^+] + [V^-] \qquad (3)$$

$$[I] = Z_0^{-1}([V^+] - [V^-]). \qquad (4)$$

From (1) and (2), the spiral-inductor Q factor can be rewritten as

$$Q_{ind} = \frac{\mathrm{Im}\{P_{av}\}}{\mathrm{Re}\{P_{av}\}}. \qquad (5)$$

After substituting (3) and (4) into (2), we can expand P_{av} in terms of the incident voltage waves ($[V^+]$) and reflected voltage waves ($[V^-]$) with corresponding real and imaginary parts given as

$$\begin{aligned}\mathrm{Im}\{P_{av}\} &= (2jZ_0)^{-1}([V^-]^t[V^+]^* - [V^+]^t[V^-]^*) \\ &= (2jZ_0)^{-1}([V^+]^t[S]^t[V^+]^* - [V^+]^t[S]^*[V^+]^* \\ &= (2Z_0)^{-1}[V^+]^t\{j^{-1}([S]^t - [S]^*)\}[V^+]^* \end{aligned} \qquad (6)$$

$$\begin{aligned}\mathrm{Re}\{P_{av}\} &= (2Z_0)^{-1}([V^+]^t[V^+]^* - [V^-]^t[V^-]^*) \\ &= (2Z_0)^{-1}([V^+]^t[U][V^+]^* - [V^+]^t[S]^t[S]^*[V^+]^*) \\ &= (2Z_0)^{-1}[V^+]^t([U] - [S]^t[S]^*)[V^+]^* \end{aligned} \qquad (7)$$

where $[U]$ is an identity matrix. Dividing (6) by (7) gives the Q factor as

$$Q_{ind} = \frac{[V^+]^t\{j^{-1}([S]^t - [S]^*)\}[V^+]^*}{[V^+]^t([U] - [S]^t[S]^*)[V^+]^*}. \qquad (8)$$

From the definition of S parameters and the facts that $V_1 = V_1^+ + V_1^-$ and $V_2^+ = \Gamma_L V_2^-$ where Γ_L represents the reflection coefficient seen looking toward the load, we have

$$V_1^- = S_{11}V_1^+ + S_{12}V_2^+ = V_1 - V_1^+ \qquad (9)$$

$$V_2^- = S_{21}V_1^+ + S_{22}V_2^+ = V_2^+ / \Gamma_L. \qquad (10)$$

Solving for V_1^+ and V_2^+ from (9) and (10) gives

$$[V^+] = \begin{bmatrix} V_1^+ \\ V_2^+ \end{bmatrix} = V_q \begin{bmatrix} F_1 \\ F_2 \end{bmatrix} \qquad (11)$$

where

$$V_q = \frac{V_1}{(1+S_{11})(1-\Gamma_L S_{22}) + \Gamma_L S_{12}S_{21}} \qquad (12)$$

$$F_1 = 1 - S_{22}\Gamma_L \qquad (13)$$

$$F_2 = S_{21}\Gamma_L. \qquad (14)$$

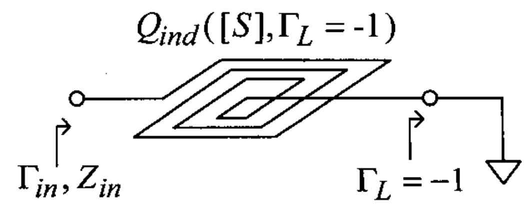

Fig. 2. A spiral inductor with a short-circuit termination.

Solving for V_1^- / V_1^+ from (9) gives

$$\begin{aligned}\Gamma_{in} &= \frac{V_1^-}{V_1^+} = S_{11} + S_{12}\frac{V_2^+}{V_1^+} = S_{11} + S_{12}\frac{F_2}{F_1} \\ &= S_{11} + \frac{S_{12}S_{21}\Gamma_L}{1 - S_{22}\Gamma_L}. \end{aligned} \qquad (15)$$

After substituting (11) into (8) and assuming the spiral inductor to be reciprocal, the spiral-inductor Q factor can be finally formulated as

$$Q_{ind} = \frac{2\,\mathrm{Im}\{S_{11}\}|F_1|^2 + 2\,\mathrm{Im}\{S_{22}\}|F_2|^2 + 4\,\mathrm{Im}\{S_{21}\}\mathrm{Re}\{F_1F_2^*\}}{[\,(1-|S_{11}|^2 - |S_{21}|^2)|F_1|^2 + (1-|S_{22}|^2 - |S_{12}|^2)|F_2|^2 - 2\,\mathrm{Re}\{(S_{11}S_{12}^* + S_{21}S_{22}^*)(F_1F_2^*)\}\,]}. \qquad (16)$$

In (16) the Q factor has been explicitly expressed in terms of the two-port S parameter and load reflection coefficient.

III. Case Study

A. Spiral Inductors with a Short-Circuit Termination

Fig. 2 shows a spiral inductor with the second port grounded. For this special case, the load reflection coefficient corresponds to $\Gamma_L = -1$ and the spiral-inductor Q factor in (16) reduces to

$$Q_{ind} = \frac{2\,\mathrm{Im}\{S_{11}\}|1+S_{22}|^2 - 2\,\mathrm{Im}\{S_{12}S_{21}(1+S_{22}^*)\}}{(1-|S_{11}|^2)|1+S_{22}|^2 - |S_{12}S_{21}|^2 + 2\,\mathrm{Re}\{S_{11}S_{12}^*S_{21}^*(1+S_{22})\}}. \qquad (17)$$

For example, five spiral inductors of different turns, N=2.5, 3.5, 4.5, 5.5, and 6.5, in 0.25 μm RF CMOS process have been measured with two-port S parameters. Their layout parameters include 10-μm width, 2-μm spacing, and 120-μm inner dimension. The metal thickness is 1.5 μm. Their Q factors are calculated using (17) and shown in Fig. 3. It can be seen that the peak values of Q factors range from 7.2 to 14.2 and basically decrease as the number of turns increases.

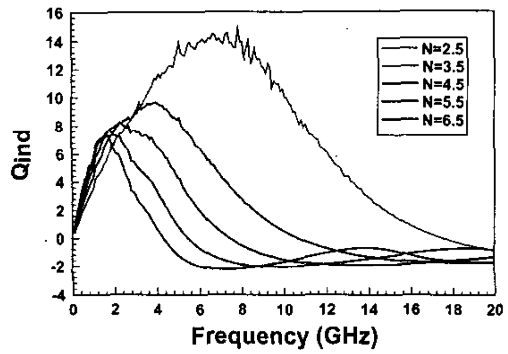

Fig. 3. Calculated Q factors for spiral inductors of different turns under short-circuit termination.

The expression of (17) can be further proved identical to the conventional Q-factor formulation based on one-port configuration. Dividing both numerator and denominator in (17) by $|1+S_{22}|^2$ gives

$$Q_{ind}=\frac{2\,\mathrm{Im}\{S_{11}\}-2\,\mathrm{Im}\{\frac{S_{12}S_{21}}{1+S_{22}}\}}{1-(|S_{11}|^2-\frac{S_{11}S_{12}^*S_{21}^*}{1+S_{22}^*}-\frac{S_{11}^*S_{12}S_{21}}{1+S_{22}}+\frac{|S_{12}S_{21}|^2}{|1+S_{22}|^2})}$$

$$=\frac{2\,\mathrm{Im}\{S_{11}-\frac{S_{12}S_{21}}{1+S_{22}}\}}{1-|S_{11}-\frac{S_{12}S_{21}}{1+S_{22}}|^2}=\frac{2\,\mathrm{Im}\{\Gamma_{in}\}}{1-|\Gamma_{\mathrm{in}}|^2}$$

$$=\frac{\mathrm{Im}\{(1+\Gamma_{in})(1-\Gamma_{in}^*)\}}{\mathrm{Re}\{(1+\Gamma_{in})(1-\Gamma_{in}^*)\}}. \quad (18)$$

By further dividing both numerator and denominator in (18) by $|1-\Gamma_{in}|^2$ and using the general relation, $Z_{in}=Z_0(1+\Gamma_{in})/(1-\Gamma_{in})$, between input impedance and reflection coefficient, we can find

$$Q_{ind}=\frac{\mathrm{Im}\{(1+\Gamma_{in})/(1-\Gamma_{in})\}}{\mathrm{Re}\{(1+\Gamma_{in})/(1-\Gamma_{in})\}}=\frac{\mathrm{Im}\{Z_{in}\}}{\mathrm{Re}\{Z_{in}\}} \quad (19)$$

which is identical to the most commonly used Q-factor expression for spiral inductors.

B. LC Tank Circuits Containing a Spiral Inductor

The definition in (1) shows that Q factor in an inductor is proportional to the net reactive energy stored, which is equal to the difference between the peak magnetic and electric energies. Due to some extra parasitic capacitances, a spiral inductor has a self-resonance at the angular frequency ω_0 when the electric and magnetic energies are equal. Therefore, its Q factor will vanish to zero at ω_0.

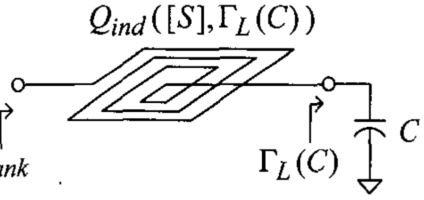

Fig. 4. A series LC tank circuit containing a spiral inductor.

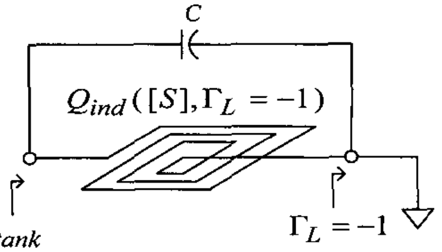

Fig. 5. A parallel LC tank circuit containing a spiral inductor.

For a tank circuit, its Q factor is proportional to the peak magnetic or electric energy at the angular tank resonant frequency (ω_r) instead. One can determine ω_r by searching for the root of imaginary part of input reflection coefficient, i.e. $\mathrm{Im}\{\Gamma_{in}(\omega_r)\}=0$. Assuming that the spiral inductor causes the dominant loss in a tank circuit, we can approximate the ratio between tank-circuit and spiral-inductor Q factors at ω_r to the form

$$\frac{Q_{\mathrm{tank}}}{Q_{ind}|_{\omega_r}}\approx\frac{2W_m^{av}|_{\omega_r}}{2W_m^{av}|_{\omega_r}-2W_e^{av}|_{\omega_r}}=\frac{1}{1-W_e^{av}|_{\omega_r}/W_m^{av}|_{\omega_r}}. \quad (20)$$

If only fundamental effects are considered, an equivalent simple parallel RLC circuit can represent a spiral inductor. Under fixed AC supply voltage, its time-average magnetic energy is proportional to $1/\omega^2$ while its electric energy is constant with frequency. With the fact that the magnetic and electric energies stored in a spiral inductor are equal at ω_0, (20) can be further approximated as

$$\frac{Q_{\mathrm{tank}}}{Q_{ind}|_{\omega_r}}\approx\frac{1}{1-W_m^{av}|_{\omega_0}/W_m^{av}|_{\omega_r}}\approx\frac{1}{1-(\omega_r/\omega_0)^2}. \quad (21)$$

Thus we can use (21) to predict Q_{tank} with the determined quantities of ω_0, ω_r and Q_{ind} at ω_r. In Figs. 4 and 5 a spiral inductor connects a lossless capacitor with variable capacitance to form a series and parallel LC tank circuit respectively. For demonstration, a 3.5-turn spiral inductor that appeared in the former case has been used. Its inductance extracted at low frequencies is about 5.9 nH.

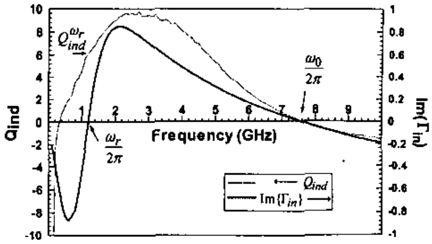

Fig. 6. The frequency responses of spiral-inductor Q factor and imaginary part of input reflection coefficient in a series LC tank circuit.

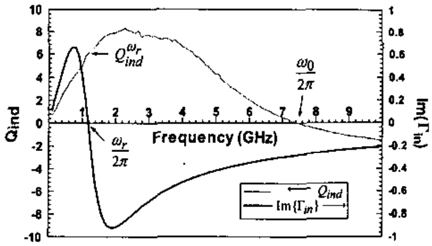

Fig. 7. The frequency responses of spiral-inductor Q factor and imaginary part of input reflection coefficient in a parallel LC tank circuit.

One should caution that the spiral inductor is treated with a capacitive termination in a series LC tank circuit but with a short-circuit termination in a parallel LC tank circuit in calculating its Q factor using (16). As a result, Figs. 6 and 7 plot the calculated Q factors versus frequency up to 10 GHz for the 5.9 nH spiral inductor connected with an ideal 3-pF capacitor in series and in parallel respectively. In addition, the resulting frequency responses of imaginary part of input reflection coefficient are also shown. From these plots, one can locate ω_0 and ω_r at which $Q_{ind} = 0$ and $\mathrm{Im}\{\Gamma_{in}\} = 0$ respectively, and then find Q_{ind} at ω_r. With knowledge of these quantities, subsequent estimation of Q_{tank} using (21) can be done. Another estimation of Q_{tank} is from the inverse of −3 dB fractional bandwidth of the simulated input admittance response. Comparisons of both estimated Q_{tank} values in a series and parallel LC tank circuit under various capacitances are shown in Figs. 8 and 9 respectively. Excellent agreement can be found.

IV. Conclusions

A closed-form S-parameter formulation of Q factor for a spiral inductor in generalized two-port configuration has been derived. The formulation can rigorously evaluate Q factor for a spiral inductor terminated with arbitrary load impedance. Therefore, the conventional Q-factor formula based on a short-circuit termination is its special case. The formulation can be also expanded to predict Q factors of tank circuits containing spiral inductors quite accurately.

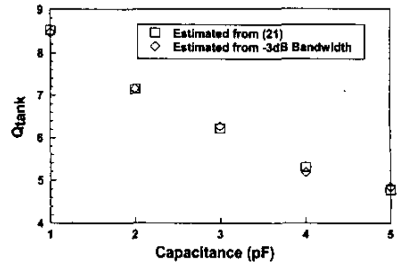

Fig. 8. Comparison of the estimated Q factors in a series LC tank circuit.

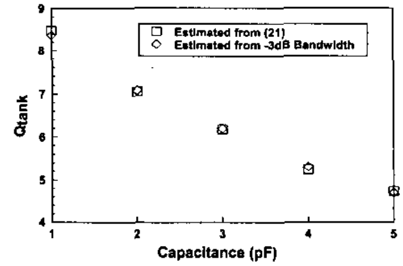

Fig. 9. Comparison of the estimated Q factors in a parallel LC tank circuit.

V. Acknowledgments

This work was supported by the ROC MOE Program for promoting academic excellence of Universities under the grant number 甲 91-E-FA08-1-4.

References

[1] C.P. Yue and S.S. Wong, "On-chip spiral inductors with patterned ground shields for Si-based RFIC's," *IEEE J. Solid-State Circuits*, vol. 33, pp. 743-752, May 1998.

[2] K.O, "Estimation methods for quality factors of inductors fabricated in silicon integrated circuit process technologies," *IEEE J. Solid-State Circuits*, vol. 33, pp. 1249-1252, Aug. 1998.

[3] H. Jiang, Y. Wang, J.A. Yeh, and N.C. Tien, "On-chip spiral inductors suspended over deep copper-lined cavities," *IEEE Trans. Microwave Theory and Tech.*, vol. 48, pp. 2415-2423, Dec. 2000.

[4] Y.E. Chen, D. Heo, J. Laskar, and T. Anderson, "Investigation of Q enhancement for inductors processed in BiCMOS technology," in *Proc. IEEE RAWCON*, 1999, pp. 263-266.

[5] K. Naishadham and T. Durak, "Measurement-based closed-form modeling of surface-mounted RF components," *IEEE Trans. Microwave Theory Tech.* vol. 50, pp. 2276-2286, Oct. 2002.